Clinical and Experimental Dermatology, 2026, 51, 1247–1254
https://doi.org/10.1093/ced/llag037
Published: 13 February 2026
Original article

CED OXFORD
Clinical and Experimental Dermatology

Improving basal cell carcinoma subtype diagnosis with dermoscopy and reflectance confocal microscopy: a multicentre prospective study

Stefania Guida[1,2] Marco Spadafora[3,4] Silvana Ciardo,[5] Marica Mirra,[4] Serena Magi,[6] Laura Mazzoni,[6] Shaniko Kaleci,[3] Francesca Farnetani,[5] Franco Rongioletti,[1,2] Ignazio Stanganelli,[6,7] Giovanni Pellacani[8] and Caterina Longo[3,5]

[1]School of Medicine, Vita-Salute San Raffaele University, Milan, Italy
[2]Dermatology Clinic, IRCCS San Raffaele Scientific Institute, Milan, Italy
[3]Department of Surgery, Medicine, Dental Medicine and Morphological Sciences, University of Modena and Reggio Emilia, Modena, Italy
[4]Azienda Unità Sanitaria Locale, IRCCS di Reggio Emilia, Skin Cancer Center, Reggio Emilia, Italy
[5]Dermatology Department, Azienda Ospedaliero-Universitaria Policlinico di Modena, Italy
[6]Skin Cancer Unit, IRCCS, Istituto Romagnolo per lo Studio dei Tumori (IRST) 'Dino Amadori', Meldola
[7]Dermatology Unit, Department of Medicine and Surgery, University of Parma, Parma, Italy
[8]Dermatology Clinic, Department of Clinical Internal, Anesthesiological and Cardiovascular Sciences, Sapienza University of Rome, Rome, Italy
Giovanni Pellacani and Caterina Longo share co-seniorship.

Correspondence: Marco Spadafora. Email: marco.spadafora@unimore.it

Abstract

Background **Basal cell carcinoma (BCC) is the most prevalent form of skin cancer. Accurate histological subtyping is essential for appropriate therapeutic planning, particularly for infiltrative variants associated with higher recurrence rates. Noninvasive imaging modalities such as dermoscopy and reflectance confocal microscopy (RCM) may enhance the diagnostic precision of BCC subtyping prior to treatment.**

Objectives **To validate dermoscopic criteria and identify RCM features associated with distinct BCC subtypes in a larger cohort and to improve the accuracy of noninvasive BCC subtyping and support precision treatment planning.**

Methods **This was a prospective multicentre study conducted between August 2017 and June 2019 across three centres in Northern Italy. In total, 281 histologically confirmed BCCs from 256 patients were analysed. Each lesion underwent standardized clinical, dermoscopic and handheld RCM evaluation prior to biopsy. Subtype-specific features were recorded and correlated with histopathology. Interobserver agreement was assessed using Cohen's kappa, and diagnostic performance was evaluated via sensitivity, specificity and the area under the receiver operating characteristic curve (AUC). The study was registered at Clinicaltrials.gov (NCT04789421).**

Results **Among the 281 BCCs, 15% were superficial, 38% were nodular and 47% were infiltrative. Dermoscopically, superficial BCCs exhibited brown globules and shiny white–red structureless areas; nodular BCCs presented blue structures, arborizing vessels and ulceration; infiltrative BCCs showed white porcelain areas and lacked pigmentation. RCM identified streaming and cords in superficial BCCs ($P = 0.003$; threefold risk), large tumour islands in nodular BCCs, and dark silhouettes in infiltrative BCCs ($P = 0.005$; two–threefold risk). Diagnostic accuracy improved with combined dermoscopy and RCM. Sensitivity for superficial BCC increased from 74.4% [95% confidence interval (CI) 60.2–85.8] to 81.4% (95% CI 68.1–91.0), specificity from 97.9% (95% CI 95.5–99.5) to 98.3% (95% CI 96.1–99.5), and AUC reached 0.899.**

Conclusions **The integration of dermoscopic and RCM findings significantly enhances the noninvasive preoperative classification of BCC subtypes. This approach improves diagnostic accuracy and may inform more precise, subtype-tailored management, reducing treatment failures and supporting personalized dermatological care.**

Accepted: 17 January 2026

What is already known about this topic?

- Dermoscopy and reflectance confocal microscopy (RCM) are established tools for diagnosing basal cell carcinoma (BCC), but their role in accurately subtyping BCC prior to treatment has been limited and based on small, retrospective cohorts.

What does this study add?

- This large, prospective multicentre study validates specific dermoscopic and RCM criteria for BCC subtypes and shows that their combined use significantly improves diagnostic accuracy and subtype classification.

Surgical excision represents the first-line treatment for basal cell carcinoma (BCC).[1] However, as the most common form of skin cancer, BCC may also be managed with nonsurgical therapies in selected cases, particularly for low-risk superficial subtypes or in older patients with comorbidities.[2]

Therefore, accurate pretreatment subtyping of BCC is essential for optimal patient management. While histopathology remains the gold standard for subtype classification, noninvasive diagnostic tools can provide rapid, bedside assessments to guide treatment decisions.[3]

BCC diagnosis typically relies on a combination of clinical and dermoscopic evaluation, which has demonstrated a diagnostic sensitivity of 93%.[4] A recent systematic review of 5950 BCCs summarized dermoscopic features by subtype but reported significant heterogeneity across studies.[5] Notably, the ability to distinguish superficial BCCs from other subtypes showed a sensitivity of only 82%.[3]

Reflectance confocal microscopy (RCM) is an advanced imaging modality that enables *in vivo* visualization of cellular and architectural skin features. Although RCM has been widely applied to BCC diagnosis, only a limited number of studies – typically involving up to 123 lesions – have explored its role in subtype classification compared with histopathology.[3,6,7]

This prospective, multicentre study aims to validate dermoscopic criteria and identify RCM features associated with distinct BCC subtypes in a larger cohort. By doing so, we seek to improve the accuracy of noninvasive BCC subtyping and support precision treatment planning.

Patients and methods

This is a prospective and multicentre study conducted at three Northern Italy centres: the Skin Cancer Center of Istituto di Ricovero e Cura a Carattere Scientifico of Reggio Emilia, the Dermatology Department of the University of Modena and Reggio Emilia, and the Skin Cancer Unit of Istituto Romagnolo per lo Studio dei Tumori and Ravenna Hospital, Ravenna-Forlì.

All centres involved shared standardized patient access and treatment protocols, in accordance with national and regional healthcare regulations. This pivotal study included all consecutive lesions clinically and dermoscopically suspected to be BCCs, assessed between August 2017 and June 2019. Inclusion criteria for the current study were the histopathological diagnosis of BCC, including subtype classification, as well as clinical, dermatoscopic and RCM images of the lesion. Exclusion criteria included hyperkeratotic or fully ulcerated lesions; no anatomical site was excluded provided that the lesion was assessable by both dermoscopy and RCM. This design ensured a robust and standardized dataset for evaluating diagnostic accuracy across imaging modalities. Patients provided written informed consent prior to participation. The study was approved by the local ethics committee (protocol number 3844/C.E.) and registered at Clinicaltrials.gov (NCT04789421).

Basal cell carcinoma subtype definition

Histopathological BCC subtype classification was performed according to a standardized, simplified scheme, categorizing tumours as superficial, nodular or infiltrative. The infiltrative category encompassed infiltrating, sclerosing and micronodular subtypes, in line with a recent consensus classification.[8]

This prospective study included only fully excised lesions, excluding punch or shave biopsies, to ensure complete histopathological evaluation. Mixed BCC subtypes were excluded unless a predominant histological component could be clearly identified and classified.

Clinical, dermoscopy and reflectance confocal microscopy imaging

After obtaining written informed consent, clinical and dermoscopic images were collected with a dermatoscope (DermLite DL1; 3Gen, Aliso Viejo, CA, USA) mounted on a camera and RCM through the handheld tool (Vivascope 3000; MAVIG GmbH, Munich, Germany), following established imaging protocols.[3,9]

For each lesion, an expert evaluator provided a bedside diagnosis of either ‘superficial BCC’ or ‘nonsuperficial BCC’ based on the combined clinical, dermoscopic and RCM assessment. Clinical data (biological sex, age) from each patient were retrieved, and clinical images were evaluated according to skin site (head–neck, trunk, upper and lower limbs), palpability (flat, papule and plaque/nodule) and degree of pigmentation (amelanotic, lightly pigmented, dark).

Dermatoscopic variables, according to previous papers,[3,10] were taken into account: multiple blue–grey dots, large blue–grey ovoid nests/globules, leaf-like structures, concentric/spoke wheel structures, arborizing vessels, short fine telangiectasias, ulceration, multiple small erosions, multiple aggregate yellow globules, shiny white structures, milky-red structureless areas and white porcelain areas.

RCM features for BCCs include streaming of the epidermis, small tumour islands, big tumour islands, cords connected to the epidermis, dark silhouette, clefting, ulceration/erosion, peripheral

palisading, increased vascularization, collagen surrounding tumour islands and inflammation.[3,4]

All images were independently evaluated by two expert readers – one with over 10 years of experience and the other with less than 10 years – in dermoscopy and RCM. This dual-reader approach allowed for assessment of interobserver agreement and ensured consistency in feature recognition. Clinical and dermoscopic images were initially reviewed together for dermoscopy-only assessment, followed by a subsequent evaluation in which the complete set of images (clinical, dermoscopic and RCM) was provided for combined dermoscopy and RCM analysis. Evaluations were blinded to the histopathological BCC subtype diagnosis.

Statistical analysis

Statistical analyses were performed with SPSS® software version 24 (IBM, Armonk, NY, USA). Qualitative variables were summarized as absolute and relative frequencies and compared using Pearson's χ^2 test or Fisher's exact test, as appropriate. Quantitative variables were reported as mean (SD) and compared using the unpaired Student's *t*-test.

Diagnostic performance metrics, including sensitivity, specificity and 95% confidence intervals (CIs), were calculated for the diagnosis of superficial BCC using dermoscopy and RCM, both before and after the study's findings were known. Receiver operating characteristic (ROC) curves were generated, and the area under the curve (AUC) was calculated. According to established thresholds, an AUC of ≤ 0.5 is nondiscriminant, 0.7–0.8 is acceptable, 0.8–0.9 is excellent, and > 0.9 is outstanding.

Interobserver agreement for dermoscopic and RCM criteria was assessed using Cohen's kappa statistic. Cohen's kappa values were interpreted as follows: ≤ 0.2 indicated poor agreement, between 0.21 and 0.40 fair agreement, between 0.41 and 0.60 moderate agreement, between 0.61 and 0.80 substantial agreement, and $\geq$ 0.81 to 1.00 indicated almost perfect agreement.

The alpha level was set at < 0.05.

Results

Study population

Overall, 256 patients [mean (SD) age 68.5 (11.5) years, range 22–95] with 281 histopathologically confirmed BCCs were included in the current study. All patients were White and were Fitzpatrick skin types I–III. Overall, 15% were superficial BCCs, 38% were nodular and 47% were infiltrative BCCs (Table 1).

Clinical data

A slight predominance of male patients was observed, although this difference was not statistically significant. Patients older than 68 years were significantly more likely to present with nonsuperficial BCCs ($P = 0.010$), particularly when comparing superficial vs. infiltrative subtypes (Table 1).

Most of the BCCs were located on the head and neck, particularly nodular and infiltrative BCCs, while superficial BCCs were prevalent on the trunk ($P = 0.001$). Nodular BCCs appeared for the most part as papules and nodules, while superficial BCCs were flat or papules; infiltrative BCCs commonly presented as flat or nodules/plaques ($P = 0.001$) (Table 1).

Additionally, over half of all BCCs were nonpigmented with a similar distribution across all subtypes, while the clinical parameter 'dark pigmentation' was slightly more frequent in nodular BCC compared with other subtypes ($P = 0.002$) (Table 1).

Dermoscopic findings

The distribution of dermoscopic features varied significantly across BCC subtypes. Brown structures were significantly associated with superficial BCCs, compared with nodular BCCs ($P = 0.017$) and infiltrative BCCs ($P = 0.000$) (Figure 1a), and blue structures were significantly associated with nodular BCCs, compared with superficial ones ($P = 0.023$) (Figure 1c, Table 1).

Nonsuperficial BCCs frequently exhibited milky-red areas and arborizing vessels; ulceration was commonly observed in both nodular and, particularly, infiltrative subtypes (Figure 1e). Finally, shiny white–red structureless areas were significantly associated with superficial BCCs compared with nodular BCCs (Table 1).

Reflectance confocal microscopy

In the univariate analysis, specific RCM features were found to be significantly associated with BCC subtypes. Streaming of the epidermis and cords connected to the epidermis was more represented in superficial BCCs, big tumour islands in nodular BCCs and dark silhouettes in infiltrative BCCs (Table 1, Figure 1).

The multivariate logistic regression model confirmed these associations. Streaming of the epidermis was associated with a threefold increased likelihood of superficial BCC ($P = 0.003$), and cords connected to the epidermis with a twofold increased likelihood ($P = 0.040$), both compared with nodular BCCs. Furthermore, the presence of a dark silhouette was significantly associated with a two–threefold increased risk of infiltrative BCC, compared with both nodular ($P = 0.005$) and superficial subtypes ($P = 0.017$) (Table 2).

Interobserver agreement

For dermoscopic features, substantial agreement was observed for the majority of parameters, while moderate agreement was noted for multiple blue–grey dots, and fair agreement for multiple small erosions.

Regarding RCM features, moderate agreement was found for clefting and increased vascularization, whereas substantial agreement was achieved for all other evaluated features (Table 3).

Diagnostic accuracy

Diagnostic accuracy for BCC subtyping was assessed by evaluating the ability of dermoscopy and RCM to correctly identify superficial BCCs, using histopathology as the reference standard (Figure 2).

Prior to the study's findings, the combined use of dermoscopy and RCM yielded a sensitivity of 74.4% (95% CI 60.2–85.8) and a specificity of 97.9% (95% CI 95.5–99.5), with an excellent AUC of 0.821.

Following the study's analysis and refinement of diagnostic criteria, sensitivity improved to 81.4% (95% CI 68.1–91.0) and specificity increased to 98.3% (95% CI 96.1–99.5), with a corresponding AUC of 0.899, indicating a notable enhancement in diagnostic performance (Figure 2).

Table 1 Demographic, clinical and histopathological data of a total of 281 basal cell carcinomas (BCCs) included in the study

					P-values			
	Total (*n* = 281)	**sBCC (*n* = 43, 15%)**	**nBCC (*n* = 106, 38%)**	**iBCC (*n* = 132, 47%)**	**Overall**	**sBCC vs. nBCC**	**nBCC vs. iBCC**	**sBCC vs. iBCC**
Sex								
Female	115 (41)	21 (49)	45 (42)	49 (37)	0.367	0.477	0.403	0.173
Male	166 (59)	22 (51)	61 (58)	83 (63)				
Age (years)								
≤ 68	127 (45)	28 (65)	48 (45)	51 (39)	0.010*	0.028*	0.301	0.002*
> 68	154 (55)	15 (35)	58 (55)	81 (61)				
Location								
Head–neck	177 (63)	14 (33)	65 (61)	98 (74)	0.001*	0.010*	0.196	0.000*
Trunk	78 (28)	23 (53)	30 (28)	25 (19)				
Upper limbs	9 (3)	1 (2)	4 (4)	4 (3)				
Lower limbs	17 (6)	5 (12)	7 (7)	5 (4)				
Palpability								
Flat	70 (25)	19 (44)	2 (2)	49 (37)	0.001*	0.000*	0.000*	0.268
Papule	108 (38)	15 (35)	55 (52)	38 (29)				
Nodule/plaque	103 (37)	9 (21)	49 (46)	45 (34)				
Clinical pigmentation								
Amelanotic	157 (56)	28 (65)	54 (51)	75 (57)	0.002*	0.043*	0.001*	0.623
Light	76 (27)	11 (26)	22 (21)	43 (33)				
Dark	48 (17)	4 (9)	30 (28)	14 (11)				
Dermoscopy								
Multiple blue–grey dots	75 (27)	10 (23)	35 (33)	30 (23)	0.175	0.649	0.043*	0.280
Blue structures	93 (33)	11 (26)	41 (39)	41 (31)	0.242	0.023*	0.099	0.234
Brown structures	39 (14)	12 (28)	15 (14)	12 (9)	0.008*	0.017*	0.043*	0.000*
Arborizing vessels	164 (58)	8 (19)	68 (64)	88 (67)	0.001*	0.000*	0.433	0.000*
Short fine telangiectasias	39 (14)	6 (14)	9 (9)	24 (18)	0.099	0.229	0.014*	0.531
Ulceration	142 (50)	16 (37)	50 (47)	76 (58)	0.046*	0.008*	0.037*	0.000*
Multiple small erosions	41 (15)	11 (26)	13 (12)	17 (13)	0.085	0.027*	0.482	0.089
MAY globules	53 (18.9)	2 (4.7)	33 (31.1)	18 (13.6)	0.240	0.098	0.909	0.108
Shiny white–red structureless areas	174 (61.9)	25 (58.1)	94 (88.7)	55 (41.7)	0.056	0.017*	0.445	0.060
Milky-red areas	120 (42.7)	4 (9.3)	52 (49.1)	64 (48.5)	0.000*	0.000*	0.930	0.000*
White porcelain areas	50 (17.8)	1 (2.3)	29 (27.4)	20 (15.2)	0.040*	0.173	0.118	0.025*
RCM								
Streaming of the epidermis	84 (30)	20 (47)	20 (19)	44 (33)	0.002*	0.012*	0.012*	0.163
Small tumour islands	152 (54)	24 (56)	61 (58)	67 (51)	0.562	0.296	0.296	0.119
Big tumour islands	68 (24)	7 (16)	34 (32)	27 (20)	0.048*	0.041*	0.041*	0.482
Cords connected to the epidermis	116 (41)	24 (56)	35 (33)	57 (43)	0.031*	0.110	0.110	0.314
Dark silhouette	121 (43)	14 (33)	40 (38)	67 (51)	0.042*	0.045*	0.045*	0.015*
Clefting	240 (85)	35 (81)	93 (88)	112 (85)	0.592	0.522	0.522	0.605
Ulceration/erosion	171 (61)	22 (51)	69 (65)	80 (61)	0.287	0.477	0.477	0.239
Peripheral palisading	237 (84)	38 (88)	89 (84)	110 (83)	0.725	0.899	0.899	0.493
Increased vascularization	254 (90)	39 (91)	98 (92)	117 (89)	0.609	0.322	0.322	0.787
Collagen surrounding tumour islands	235 (84)	33 (77)	88 (83)	114 (86)	0.326	0.474	0.474	0.135
Inflammation	169 (60)	27 (63)	67 (63)	75 (57)	0.563	0.318	0.318	0.490

Values are *n* (%). iBCC, infiltrative BCC; MAY, multiple aggregate yellow; nBCC, nodular BCC; sBCC, superficial BCC. *$P < 0.05$ is significant

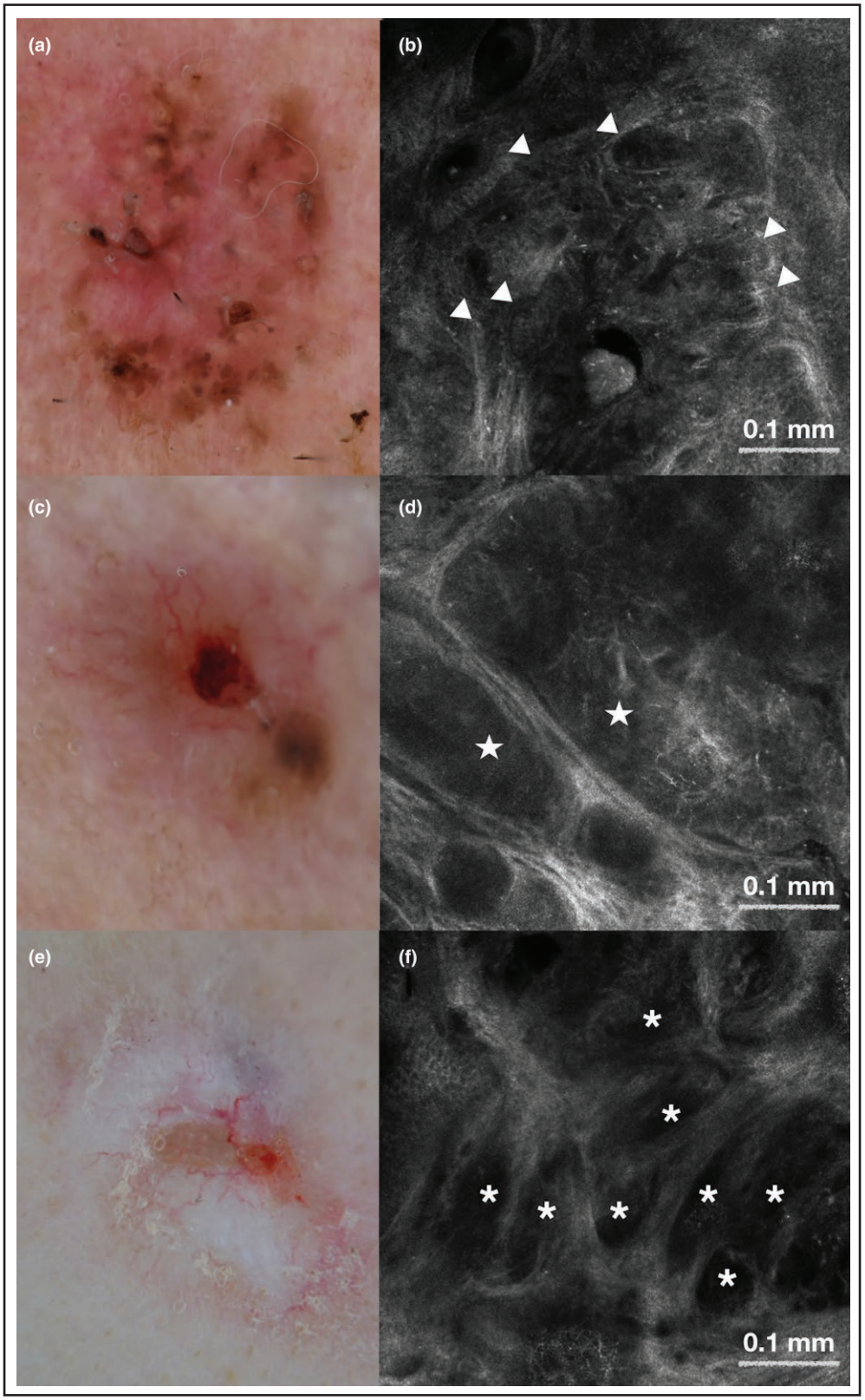

Figure 1 Dermoscopy and reflectance confocal microscopy (RCM) of (a, b) superficial basal cell carcinoma (BCC), showing (a) brown structures and shiny-red structureless areas in dermoscopy, with (b) corresponding cords in RCM (arrowheads); (c, d) nodular BCC, (c) blue structures, arborizing vessels and ulceration in dermoscopy, with (d) corresponding big tumour islands in RCM (star-shaped markers); (e, f) infiltrative BCC, (e) with porcelain areas, ulceration and arborizing vessels in dermoscopy, and (f) dark silhouette in RCM (asterisks).

Table 2 Results of multivariate analysis according to reflectance confocal microscopy features

Subtypes/variables	OR (95% CI)	*P*-value
sBCC vs. nBCC		
Streaming	0.3 (0.135–0.669)	0.003*
Cords	0.4 (0.208–0.964)	0.040*
Ulceration/erosion	1.9 (0.884–4.099)	0.100
nBCC vs. iBCC		
Streaming	0.5 (0.255–1.093)	0.085
Big tumour islands	2.3 (0.888–6.282)	0.085
Dark silhouette	3.1 (1.414–6.745)	0.005*
sBCC vs. iBCC		
Dark silhouette	2.4 (1.176–5.113)	0.017*

BCC, basal cell carcinoma; CI, confidence interval; iBCC, infiltrative BCC; nBCC, nodular BCC; OR, odds ratio; sBCC, superficial BCC. *$P < 0.05$ is significant.

Table 3 Interobserver agreement for dermoscopic and reflectance confocal microscopy features

Features	Cohen kappa
Dermoscopic	
Multiple blue–grey dots	0.518
Large blue–grey ovoid nests/globules	0.702
Brown	0.619
Arborizing vessels	0.747
Short fine telangiectasias	0.509
Ulceration	0.723
Multiple small erosions	0.401
Multiple aggregate yellow globules	0.709
Shiny white–red structures	0.760
Milky-red structureless areas	0.679
White porcelain areas	0.734
Reflectance confocal microscopy	
Streaming of the epidermis	0.737
Small tumour island	0.720
Big tumour island	0.739
Cords connected to the epidermis	0.709
Dark silhouette	0.744
Clefting	0.635
Ulceration	0.799
Peripheral palisading	0.705
Increased vascularization	0.586
Collagen surrounding tumour islands	0.708
Inflammation	0.760

Discussion

This prospective, multicentre study identified significant differences in clinical, dermoscopic and RCM characteristics across BCC subtypes, underscoring how the integration of RCM with dermoscopy can markedly improve preoperative subtype classification and enhance diagnostic accuracy. Other emerging noninvasive imaging techniques, such as line–field confocal optical coherence tomography, have already demonstrated their usefulness in improving the diagnostic accuracy of BCCs.[11] The diagnostic gap between dermoscopy and histopathology represents an unmet diagnostic need, as highlighted by previous reports.[11,12]

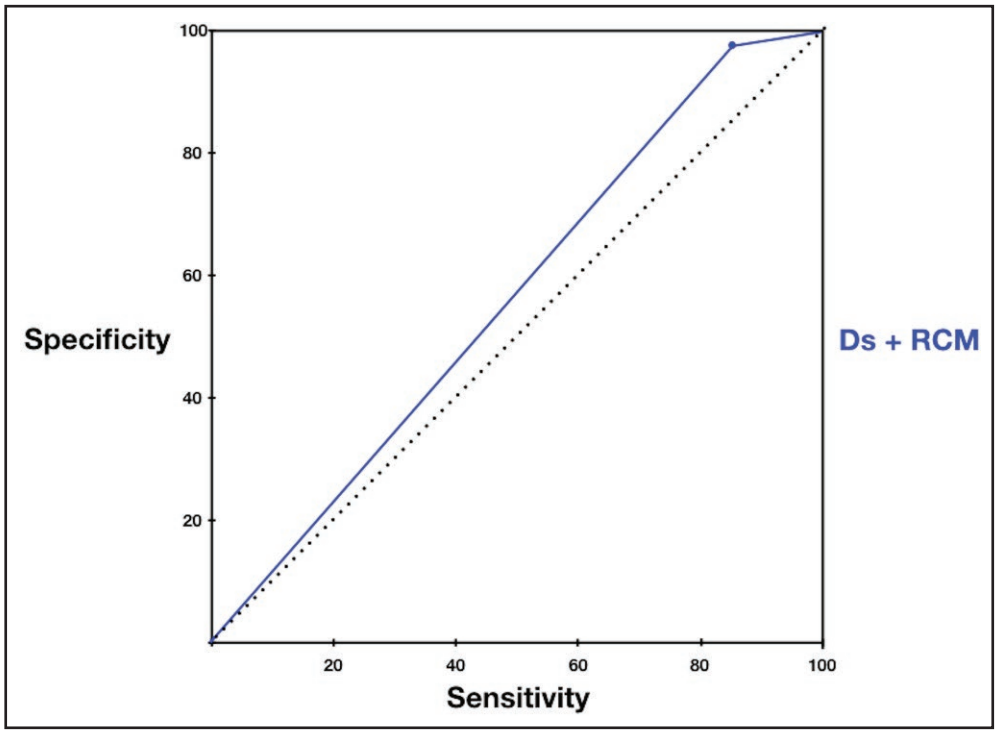

Figure 2 Receiver operating characteristic curve for dermoscopy (Ds) and reflectance confocal microscopy (RCM) and the area under the curve obtained.

Furthermore, the absence of pigmented structures poses a well-recognized diagnostic challenge.[13,14] Noninvasive diagnostic tools are therefore clinically relevant, particularly considering that up to 40% of treatment failures for superficial BCCs have been attributed to the presence of an undetected nonsuperficial component. This finding emphasizes the importance of accurate subtyping to guide appropriate therapeutic decisions.[15]

Our dermoscopic analysis revealed distinctive subtype-specific patterns: brown structures and shiny white–red structureless areas were significantly associated with superficial BCCs; blue structures, arborizing vessels and ulceration characterized nodular BCCs; and white porcelain areas and the absence of brown structures were indicative of infiltrative BCCs. These findings are consistent with prior literature and reinforce the diagnostic value of dermoscopy.[10,16–19]

RCM analysis further supported subtype differentiation. Streaming of the epidermis and cords connected to the epidermis were associated with a threefold and twofold increased likelihood, respectively, of superficial BCCs. Dark silhouettes were significantly associated with a two–threefold increased risk of infiltrative BCCs. These associations, previously suggested in a retrospective study,[3] were statistically confirmed in our prospective design.

The combined use of dermoscopy and RCM in our study achieved excellent diagnostic performance for superficial BCCs, representing a notable improvement over previous works based on dermoscopy alone. A previous study assessing the performance of dermoscopy in classifying different BCC subtypes reported lower diagnostic accuracy, further emphasizing the added diagnostic value of integrating RCM, particularly in enhancing specificity and reducing misclassification of superficial and infiltrative subtypes.[18] These findings highlight the added diagnostic value of integrating RCM, particularly in increasing specificity, which is critical for avoiding undertreatment of more aggressive subtypes. To corroborate our findings, a recent study demonstrated that RCM achieved a specificity of 88.9% for superficial BCCs, closely approaching the 91% specificity obtained from histopathological analysis on punch biopsy samples.[20]

Our results suggest that the combination of the noninvasive techniques of dermoscopy and RCM may offer a comparable diagnostic performance to biopsy in selected cases, supporting their use in preoperative planning and subtype stratification. Additionally, we observed fair to substantial interobserver agreement for both dermoscopic and RCM features, supporting the reproducibility and reliability of these criteria in clinical practice.[3]

This study has several limitations that should be acknowledged. Firstly, while RCM significantly improved diagnostic accuracy, it is inherently limited by its imaging depth, which typically reaches only the upper dermis. This constraint may reduce its sensitivity for detecting deeply infiltrative components of BCC, particularly in sclerosing or micronodular subtypes, where tumour extension may occur beyond the reach of RCM visualization.

Secondly, although interobserver agreement was generally fair to substantial, reader experience may have influenced diagnostic performance, and the study did not stratify results based on expertise level.

Additionally, some BCC subtypes, such as the superficial type, above all pigmented tumours, may be under-represented in our analysis due to their clinical management, as these lesions are often treated without histopathological confirmation.

Finally, the exclusion of mixed BCC subtypes unless a predominant component was present may have led to an under-representation of complex lesions that can be observed in clinical practice.

Taken together, our findings highlight the value of integrating dermoscopy and RCM for accurate BCC subtyping. This approach may reduce misclassification, optimize treatment selection, and support precision dermatology.

In conclusion, the results of this prospective, multicentre study suggest that the combined use of dermoscopy and RCM improves the preoperative classification of BCC subtypes.

The integration of these noninvasive diagnostic tools enhances diagnostic accuracy, particularly for superficial BCCs, where misclassification can lead to inappropriate treatment choices. This is especially important given that up to 40% of treatment failures in superficial BCCs are due to undiagnosed nonsuperficial components.

Our findings support the use of a multimodal diagnostic approach in routine clinical practice, offering a reliable, reproducible and clinically impactful method for guiding BCC management.

Future research should aim to validate these findings in broader patient populations and explore the cost-effectiveness and implementation of this approach in diverse clinical settings.

Author contributions

Stefania Guida (Conceptualization, Data curation, Formal analysis [equal]), Marco Spadafora (Data curation [equal]), Silvana Ciardo (Data curation, Writing—review & editing [equal]), Marica Mirra (Investigation [equal]), Serena Magi (Data curation [equal]), Laura Mazzoni (Data curation [equal]), Shaniko Kaleci (Formal analysis [equal]), Francesca Farnetani (Data curation [equal]), Franco Rongioletti (Supervision [equal]), Ignazio Stanganelli (Supervision [equal]), Giovanni Pellacani (Conceptualization, Supervision [equal]), and Caterina Longo (Conceptualization, Supervision [equal]).

Funding sources

Dr Marco Spadafora was partially supported by Italian Ministry for University and Research (MUR), through the PRIN 2022 Project “Cutaneous squamous cell carcinoma: stratifying high risk tumors with novel technologies” project code 2022MZEEZB (CUPE53D23013260006) National Recovery and Resilience Plan (PNRR), Italy, Mission 04 Component 2 Investment 1.1 – NextGenerationEU.

Conflicts of interest

The authors declare they have no conflicts of interest.

Data availability

The data underlying this article will be shared on reasonable request to the corresponding author.

Ethics statement

Protocol number 3844/C.E., protocol available at Clinicaltrials.gov (NCT04789421).

Patient consent

Written patient consent for publication was obtained.

References

1 Peris K, Fargnoli MC, Kaufmann R *et al.* European consensus-based interdisciplinary guideline for diagnosis and treatment of basal cell carcinoma-update 2023. *Eur J Cancer* 2023; **192**:113254.

2 Lai M, Pampena R, Mirra M *et al.* Characteristics and management of skin cancers in very elderly patients: a real-world challenge for clinicians. *Exp Dermatol* 2022; **31**:1554–62.

3 Longo C, Lallas A, Kyrgidis A *et al.* Classifying distinct basal cell carcinoma subtype by means of dermatoscopy and reflectance confocal microscopy. *J Am Acad Dermatol* 2014; **71**:716–24.e1.

4 Longo C, Guida S, Mirra M *et al.* Dermoscopy and reflectance confocal microscopy for basal cell carcinoma diagnosis and diagnosis prediction score: a prospective and multicenter study on 1005 lesions. *J Am Acad Dermatol* 2024; **90**:994–1001.

5 Reiter O, Mimouni I, Dusza S *et al.* Dermoscopic features of basal cell carcinoma and its subtypes: a systematic review. *J Am Acad Dermatol* 2021; **85**:653–64.

6 Kadouch DJ, Leeflang MM, Elshot YS *et al.* Diagnostic accuracy of confocal microscopy imaging vs. punch biopsy for diagnosing and subtyping basal cell carcinoma. *J Eur Acad Dermatol Venereol* 2017; **31**:1641–8.

7 Peppelman M, Wolberink EAW, Blokx WAM *et al. In vivo* diagnosis of basal cell carcinoma subtype by reflectance confocal microscopy. *Dermatology* 2013; **227**:255–62.

8 Fernández-Figueras MT, Malvehi J, Tschandl P *et al.* Position paper on a simplified histopathological classification of basal cell carcinoma: results of the European Consensus Project. *J Eur Acad Dermatol Venereol* 2022; **36**:351–9.

9 Castro RP, Stephens A, Fraga-Braghiroli NA *et al.* Accuracy of *in vivo* confocal microscopy for diagnosis of basal cell carcinoma: a comparative study between handheld and wide-probe confocal imaging. *J Eur Acad Dermatol Venereol* 2015; **29**:1164–9.

10 Camela E, Ilut Anca P, Lallas K *et al.* Dermoscopic clues of histopathologically aggressive basal cell carcinoma subtypes. *Medicina (Kaunas)* 2023; **59**:349.

11 Barbarossa L, D'Onghia M, Cartocci A *et al.* Understanding the dermoscopic patterns of basal cell carcinoma using line–field confocal tomography. *Tomography* 2024; **10**:826–38.

12 Cappilli S, Paradisi A, Di Stefani A *et al.* Line–field confocal optical coherence tomography: a new skin imaging technique reproducing a 'virtual biopsy' with evolving clinical applications in dermatology. *Diagnostics (Basel)* 2024; **14**:1821.

13 Ambrosio L, Pogorzelska-Antkowiak A, Retrosi C *et al.* Reflectance confocal microscopy and dermoscopy for the diagnosis of solitary hypopigmented pink lesions: a narrative review. *Cancers* 2024; **16**:2972.

14 Spadafora M, Megna A, Lippolis N *et al.* Dermoscopy and reflectance confocal microscopy of solitary flat pink lesions: a new combined score to diagnose amelanotic melanoma. *J Eur Acad Dermatol Venereol* 2025; **39**:109–16.

15 van Delft LCJ, Nelemans PJ, Jansen MHE *et al.* Histologic subtype of treatment failures after noninvasive therapy for superficial basal cell carcinoma: an observational study. *J Am Acad Dermatol* 2019; **80**:1022–8.

16 Lallas A, Apalla Z, Ioannides D *et al.* Dermoscopy in the diagnosis and management of basal cell carcinoma. *Future Oncol* 2015; **11**:2975–84.

17 Lallas A, Apalla Z, Argenziano G *et al.* The dermatoscopic universe of basal cell carcinoma. *Dermatol Pract Concept* 2014; **4**:11–24.

18 Lallas A, Tzellos T, Kyrgidis A *et al.* Accuracy of dermoscopic criteria for discriminating superficial from other subtypes of basal cell carcinoma. *J Am Acad Dermatol* 2014; **70**:303–11.

19 Conforti C, Pizzichetta MA, Vichi S *et al.* Sclerodermiform basal cell carcinomas vs. other histotypes: analysis of specific demographic, clinical and dermatoscopic features. *J Eur Acad Dermatol Venereol* 2021; **35**:79–87.

20 Woliner-van der Weg W, Peppelman M, Elshot YS *et al.* Biopsy outperforms reflectance confocal microscopy in diagnosing and subtyping basal cell carcinoma: results and experiences from a randomized controlled multicentre trial. *Br J Dermatol* 2021; **184**:663–71.